SUPPLEMENTARY MATERIAL

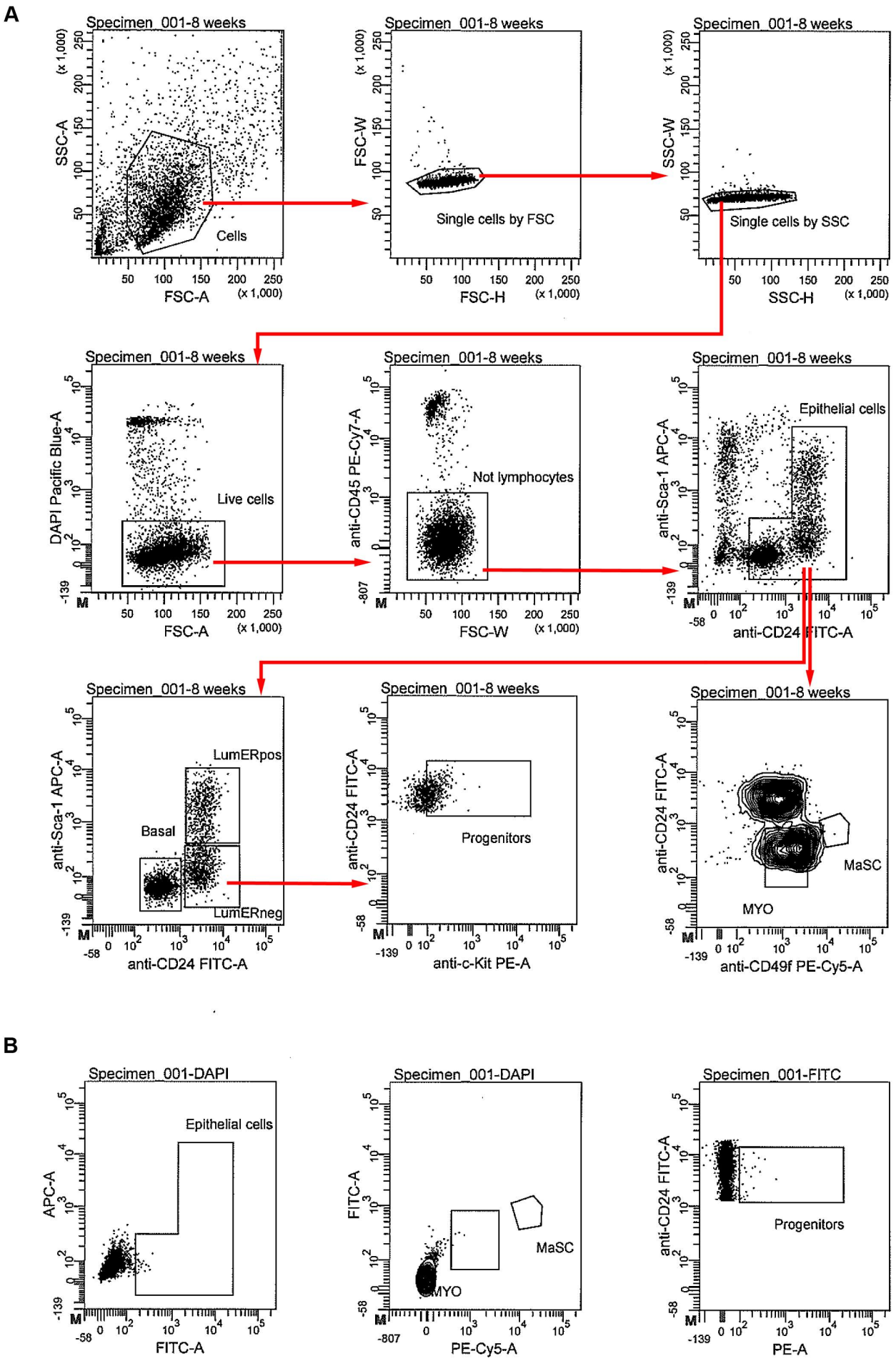

SUPPLEMENTARY FIGURE S1

Fig. S1. Flow cytometry gating workflow for isolation of mammary epithelial subpopulations. (A) Gating workflow demonstrating identification of single cells by time-of-flight analysis on forward and then side scatter, followed by exclusion of DAPI+ dead cells and CD45+ white blood cells. Remaining cells are then plotted on a Sca-1 vs CD24 plot and the epithelial cells gated as described (Britt et al., 2009). This sorting strategy isolates all mammary epithelial cells (Britt et al., 2009). The epithelial-only population is then analysed in two ways. First, it is plotted on a Sca-1 vs CD24 dot plot and the luminal ER+ and luminal ER- populations gated, with c-Kit staining of the latter being further assessed to identify the c-Kit+ progenitors. Second, the epithelial population is plotted on a CD24 vs CD49f contour plot (linear density, 5% intervals) to identify the MYOs and MaSCs, as previously described in detail (Britt et al., 2009; Soady et al., 2015). MASCs, MYOs, Luminal ER- and Luminal ER+ cells, as gated, collectively form >90% of the total mammary epithelium (Regan et al., 2012). (B) Control plots showing samples in which either only DAPI was added (left, middle) or in which the anti-c-Kit-PE was omitted (right).

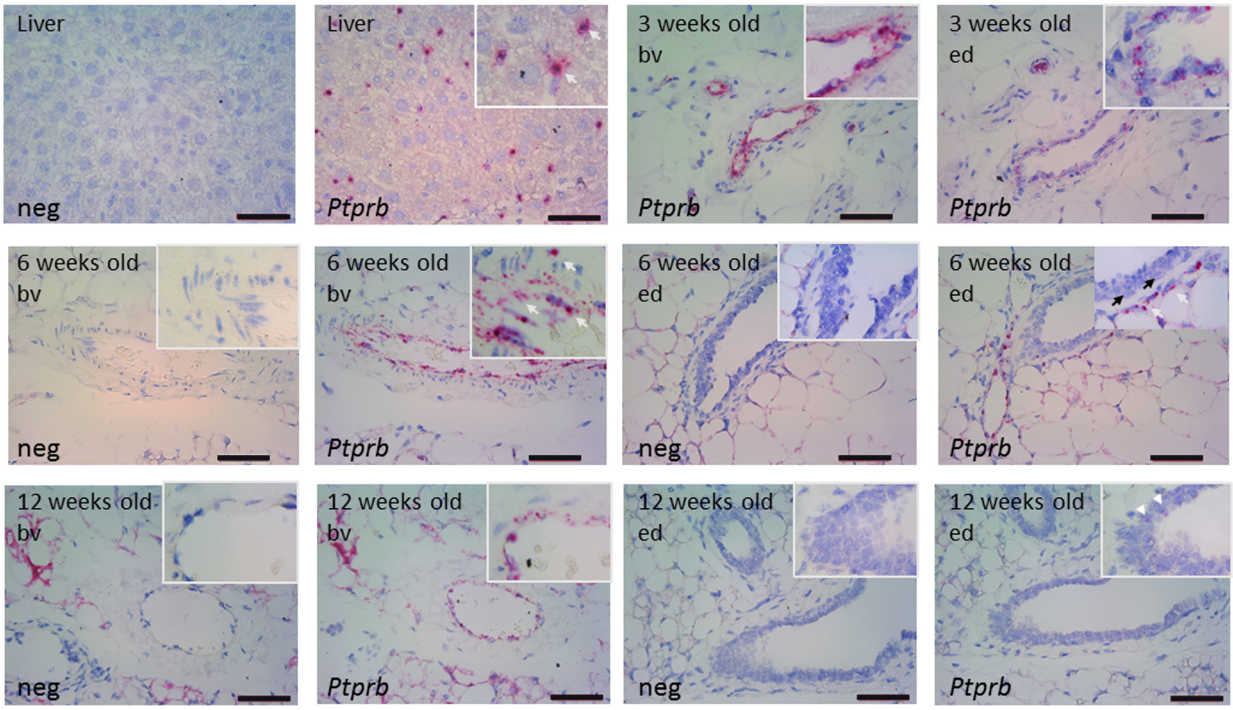

SUPPLEMENTARY FIGURE S2

Fig. S2. *Ptprb* localisation by RNAScope 2.5 HD Duplex *in situ* hybridisation. Red label indicates a positive signal. 'Neg' indicates samples labelled with the negative control probe. '*Ptprb*' indicates samples labelled with the *Ptprb* probe. 'bv' indicates a blood vessel, 'ed' epithelial duct. Bars = 50µm. Top row, liver (left two panels) used as positive control tissue, and sections from 3 week old mammary gland (right two panels). A strong, uniform *Ptprb* signal was detected on the endothelial cells lining blood vessels (middle right panel) and a positive signal was also detected in a subset of cells lining epithelial ducts (far right panel). Middle row, 6 week old mammary gland, showing a strong *Ptprb* signal on blood vessels (left two panels, white arrows on inset) and a signal on stromal cells surrounding the epithelial ducts (right panels, white arrows on inset) but no signal could be detected in the epithelium. Note that the positioning of distinctive elongated myoepithelial nuclei (black arrows on inset) demonstrate that the labelled cells are indeed outside the ducts. Bottom row, 12 week old mammary gland, again showing a strong *Ptprb* signal on blood vessels (left two panels) and a weak positive signal in a subset of cells lining epithelial ducts (right two panels, arrowheads on inset).

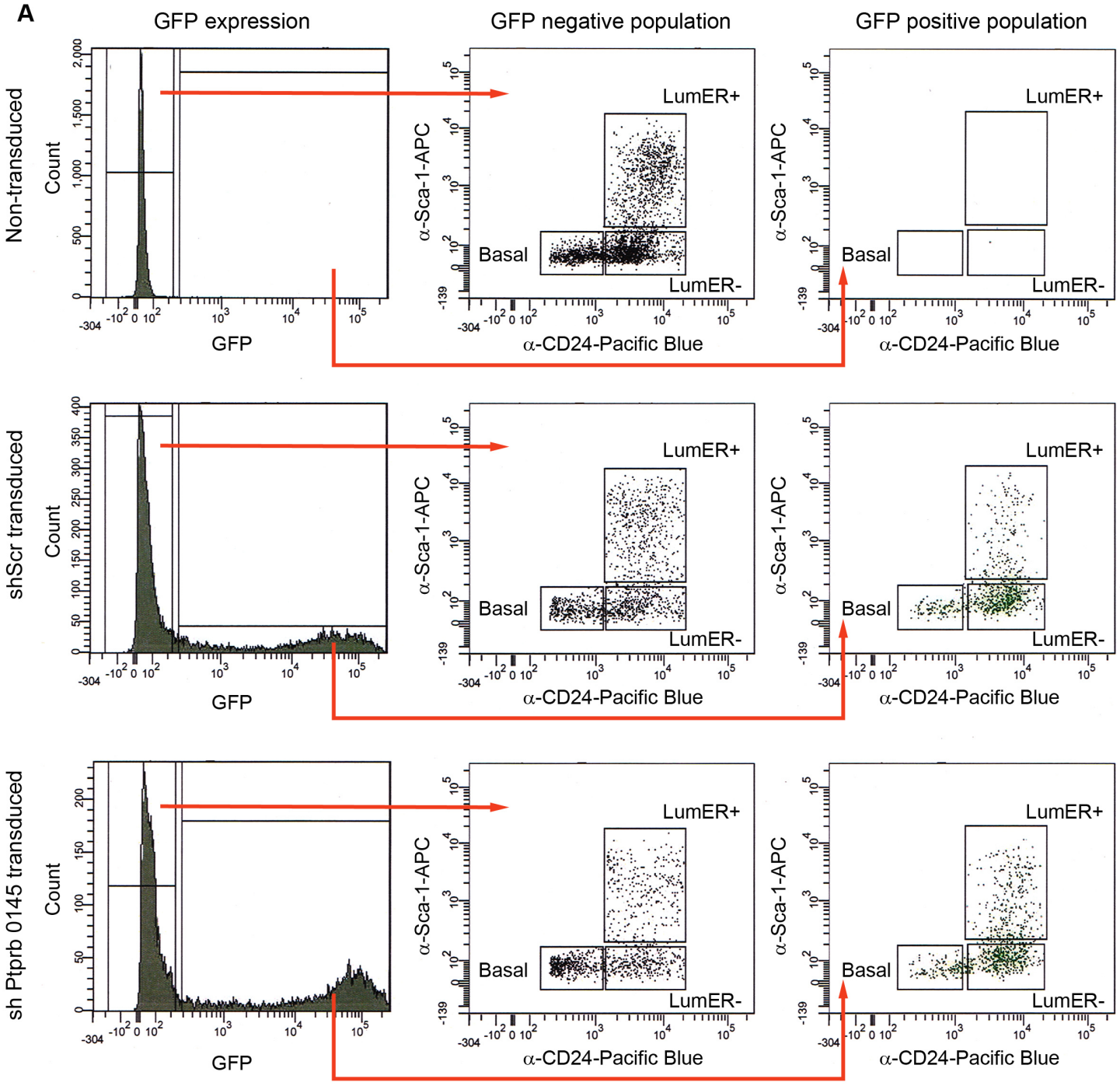

B

Percentages of epithelial subpopulations within GFP+ cells

	shScr			shPtprb 0145			shPtprb 3820		
	Mean (%)	SD (%)	n	Mean (%)	SD (%)	n	Mean (%)	SD (%)	n
Basal	11.03	3.34	6	13.73	3.35	3	16.57	10.18	3
LumERneg	55.38	5.15	6	47.87	1.99	3	47.17	4.44	3
LumERpos	28.33	4.36	6	33.30	5.84	3	29.47	6.09	3

SUPPLEMENTARY FIGURE S3

Fig. S3. *Ptprb* knockdown does not alter proportions of cell populations *in vitro*. (A) Representative flow cytometry plots form analysis of cells recovered from transplanted mammary fat pads. Only the epithelial populations are shown. Epithelial outgrowths from viral transplants consist of both transduced (GFP positive) and non-transduced cells (GFP negative) and both of these include basal, LumER- and LumER+ populations, defined by CD24 and Sca-1 expression patterns (Soady et al., 2015). Top, analysis of fat pads carrying non-transduced cells. Middle, analysis of shScr-transduced transplants. Bottom, analysis of sh Ptprb 0145-transduced transplants. **(B)** Proportions of basal, luminal ER negative and luminal ER positive cell populations in GFP+ (viral-transduced) cells harvested from fat pads transplanted with primary mammary epithelial cells transduced with shScr, shPtprb 0145 or shPtprb 3820. Data presented as mean proportion of total epithelial cells ± SD. *n* indicates number of independent transplant experiments, each of which included at least five transplanted fat pads, which contributed to the data. There are no differences between the proportions of the populations in the control compared to the knockdown transplants.

A

	Transplant Series					
	shLuc	Ptprb pool	shScr	shPtprb 0145	shScr	shPtprb 3820
Size analysis n =	8	11	9	13	14	11
Branching analysis n =	5	7	9	9	9	5

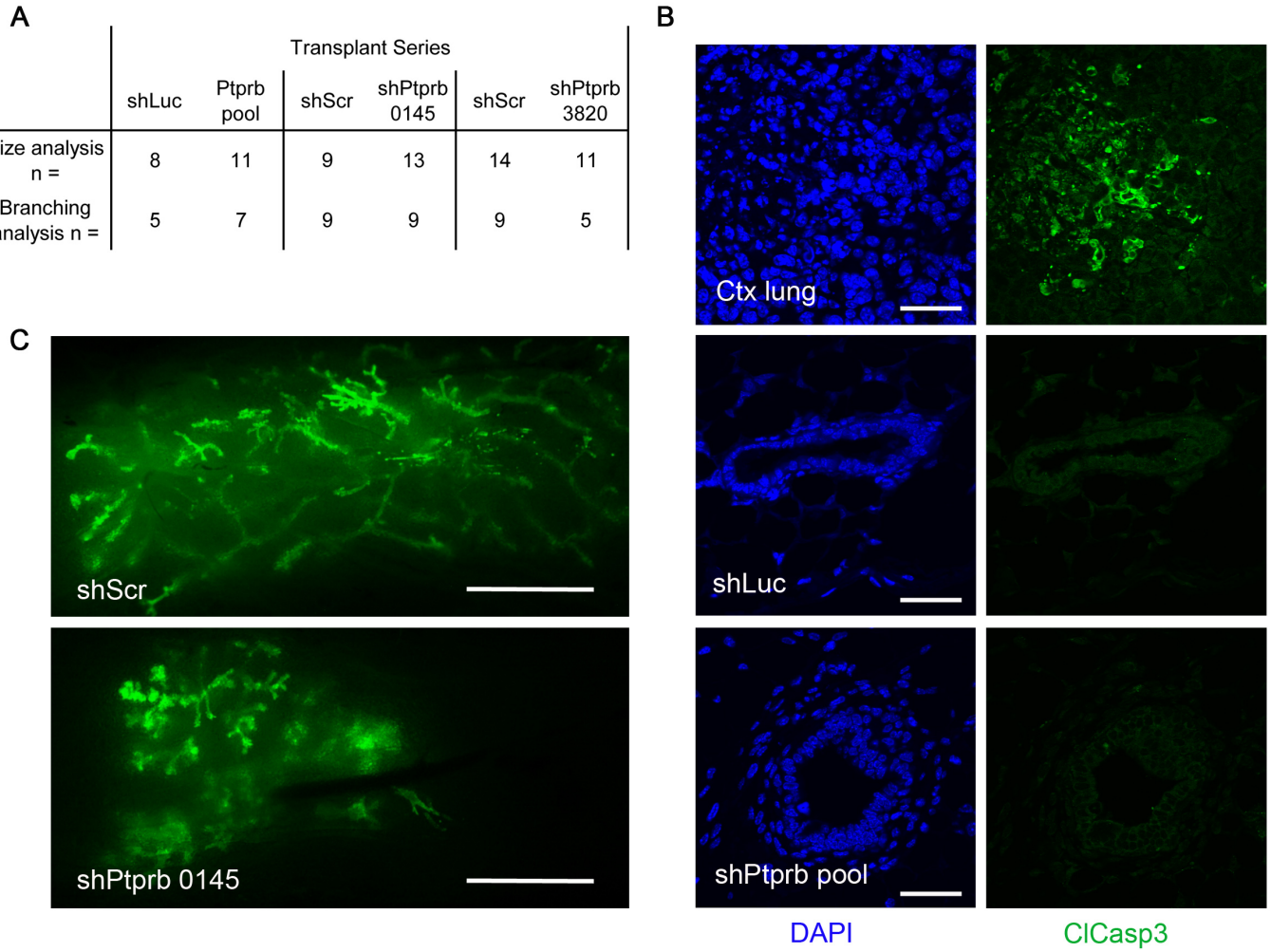

SUPPLEMENTARY FIGURE S4

Fig. S4. *Ptprb* knockdown does not enhance apoptosis. (A) Numbers of transplanted fat pads used to determine the size of outgrowths from knockdown and control cells and the amount of branching. **(B)** Cleaved Caspase-3 / DAPI staining of shLuc and shPtprb transplants, together with positive control lung tissue sample (Ctx, chemotherapy-treated). Bar = 100 μm. **(C)** Wholemounts of fat pads from secondary transplants of shScr (top) and shPtprb 0145 (bottom) transduced cells. Bars = 5 mm.

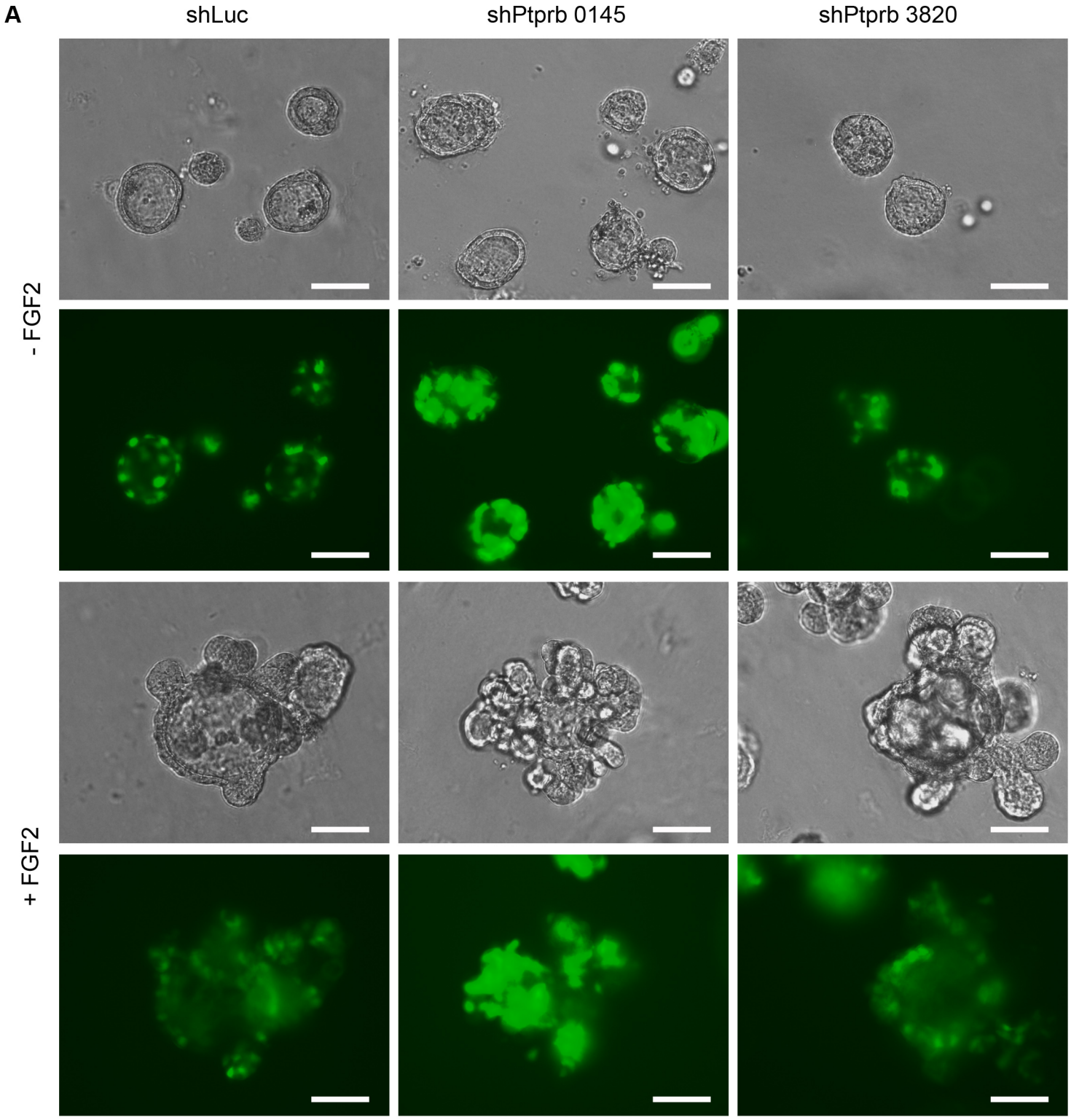

SUPPLEMENTARY FIGURE S5

Fig. S5. *In vitro* organoid branching is dependent on FGF2. (A) Transduction with shLuc, shPtprb 0145 or shPtprb 3820 in the absence of FGF2 stimulation does not cause branching. High levels of sh lentiviral transduction are indicated by strong GFP expression. Images are representative of multiple independent wells from three indpendent experiments. Paired phase contrast and GFP pictures are shown. Scale bars = 30 μm. **(B)** Examples of untreated organoids and organoids treated for seven days with 50 ng ml^{-1} FGF2, ANG1 or ANG2. Branching of organoids is only seen in FGF2 stimulated cultures. Images are representative of multiple independent wells from three independent experiments. Scale bars = 30 μm.

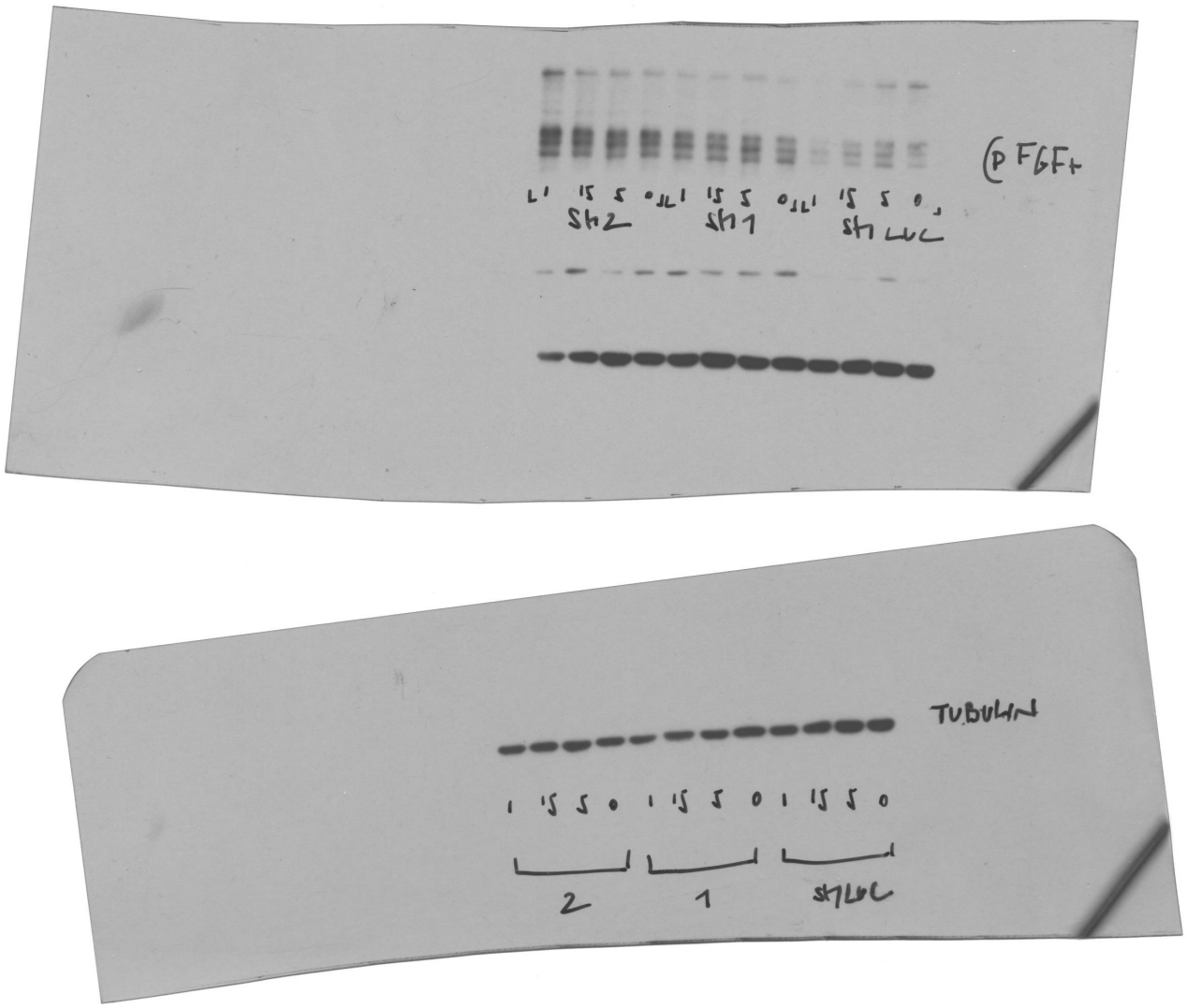

SUPPLEMENTARY FIGURE S6

Fig. S6. *Ptprb* knockdown enhances FGFR phosphorylation. Raw western blot data of effects of *Ptprb* knockdown on FGFR phosphorylation in response to FGF2 stimulation. Films of blots probed for phospho FGFR and TUBULIN are shown (blots used for preparing Figure 7A). ‘Sh1’ and ‘1’ indicate sh Ptprb 0145. ‘Sh2’ and ‘2’ indicate sh Ptprb 3820.

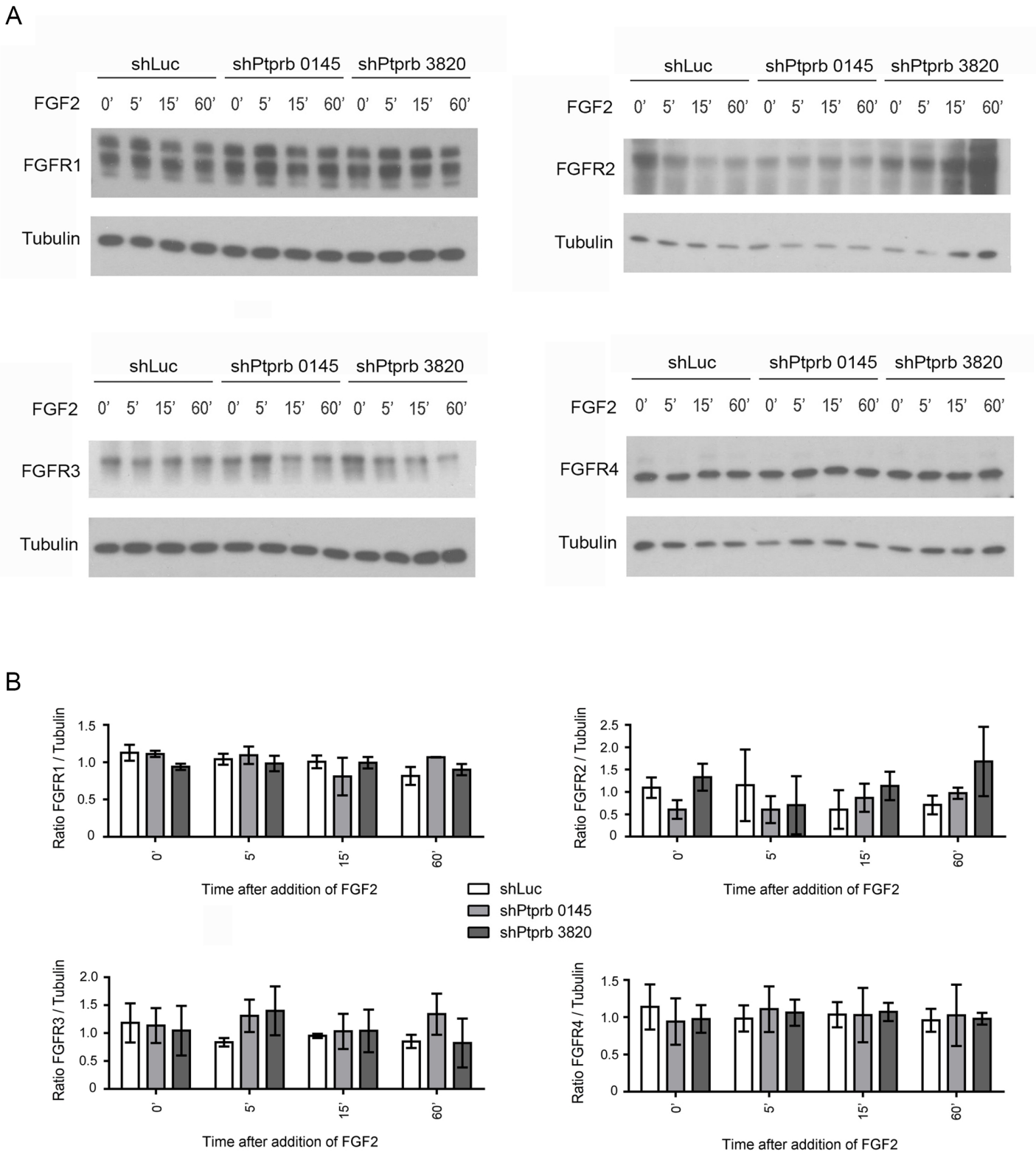

SUPPLEMENTARY DATA FIGURE S7

Fig. S7. *Ptprb* knockdown does not alter total FGFR levels. (A) Western blot analysis of total FGFR1, 2, 3 and 4 levels in organoid cultures transduced with control, 0145 or 3820 knockdown lentiviruses and either unstimulated or stimulated with FGF2. **(B)** Quantitation of total FGFR levels (mean ±SD; n=3).

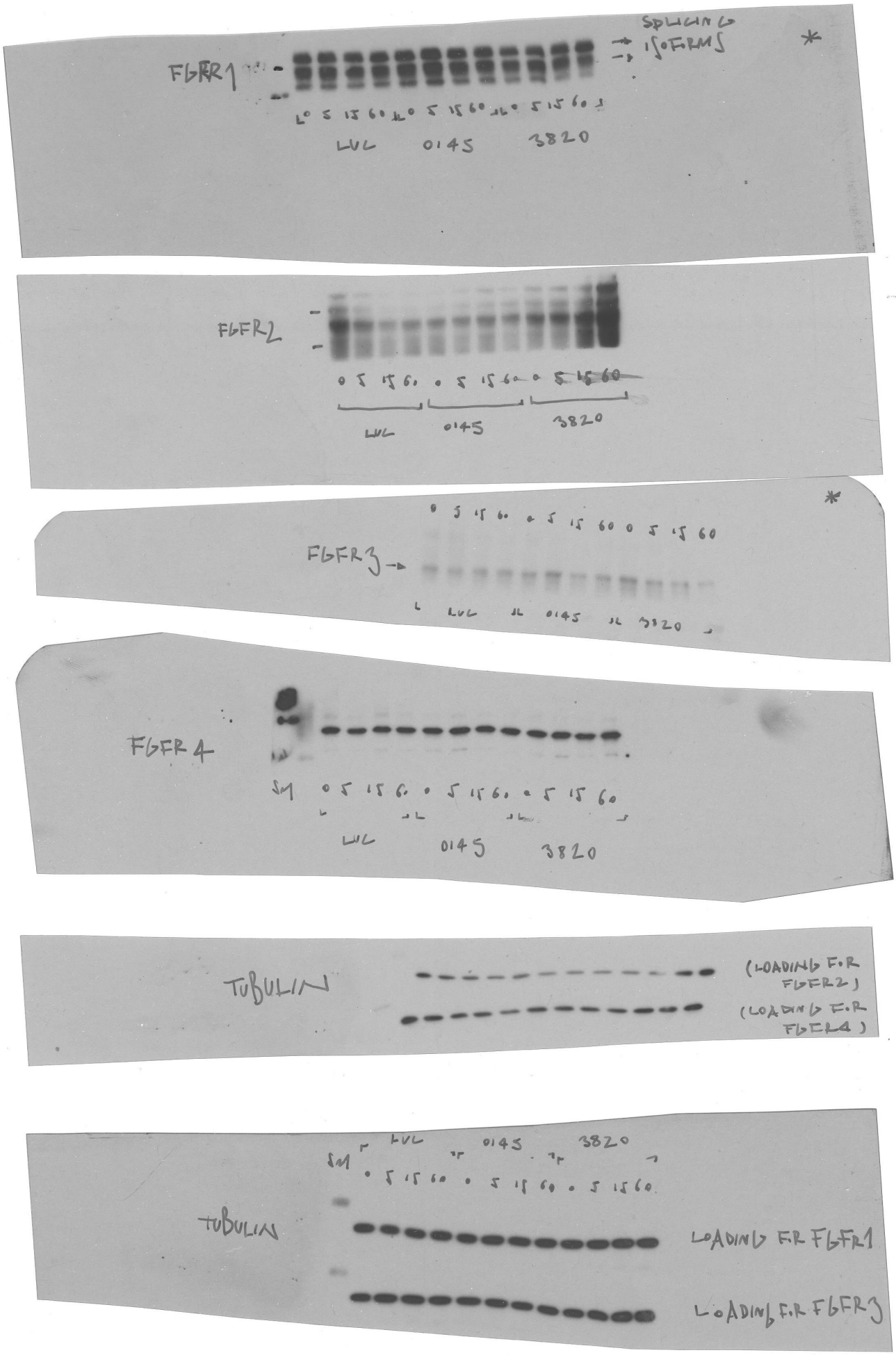

SUPPLEMENTARY FIGURE S8

Fig. S8. *Ptprb* knockdown does not alter total FGFR levels. Raw western blot data of total FGFR1, 2, 3 and 4 levels in organoid cultures transduced with control, 0145 or 3820 knockdown lentiviruses and either unstimulated or stimulated with FGF2 (blots used for preparing Supplementary Figure S7).

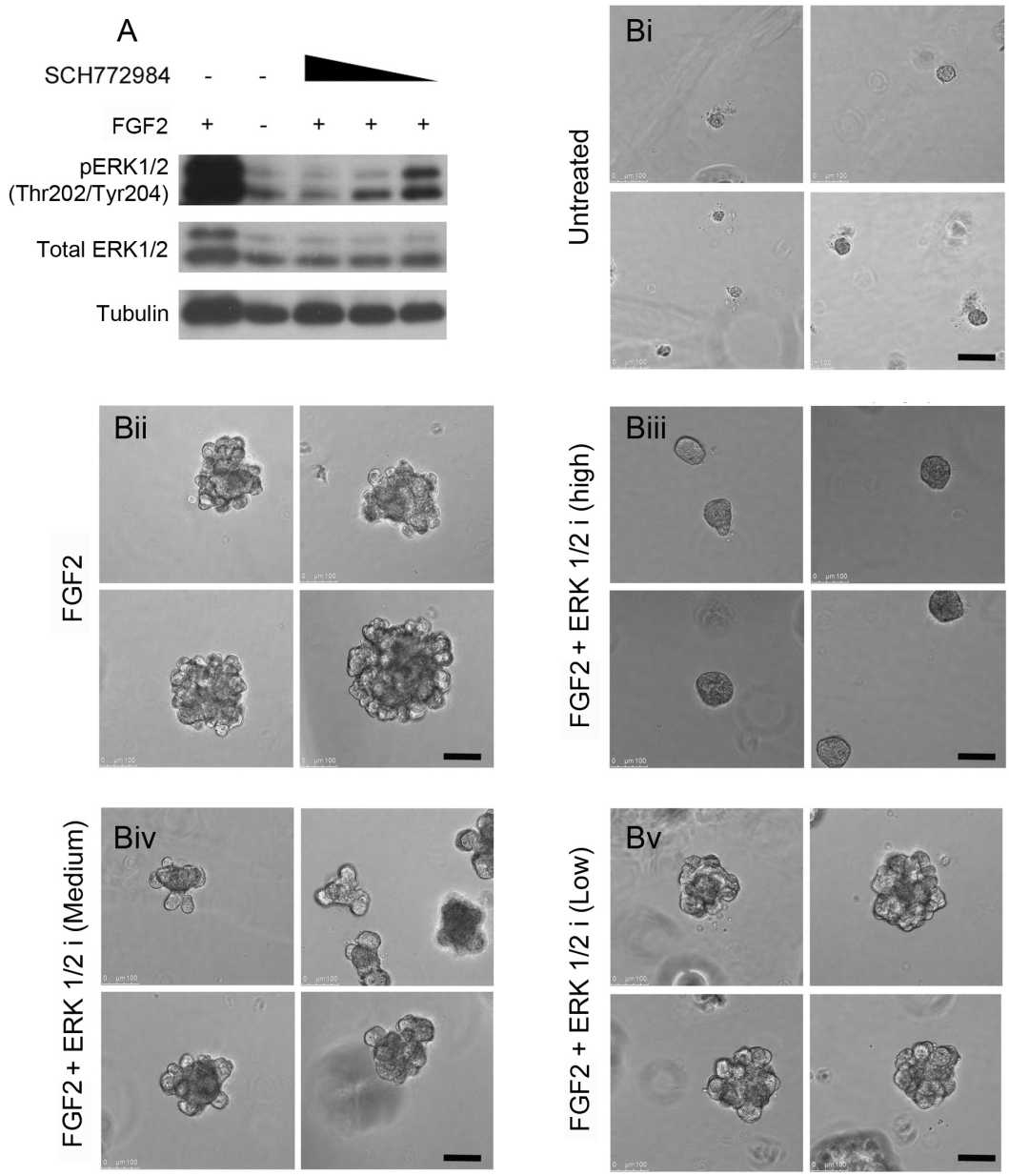

SUPPLEMENTARY FIGURE S9

Fig. S9. ERK1/2 inhibition blocks bFGF-induced mammary branching. (A) Western blot analysis of phospho- and total ERK1/2 levels in organoid cultures either unstimulated or stimulated with FGF2 and treated with High (8 nM), Medium (4 nM) or Low (2 nM) concentration of SCH772984. Tubulin was used as loading control. **(Bi - Bv)** Representative images of organoids at day 8 of culture.

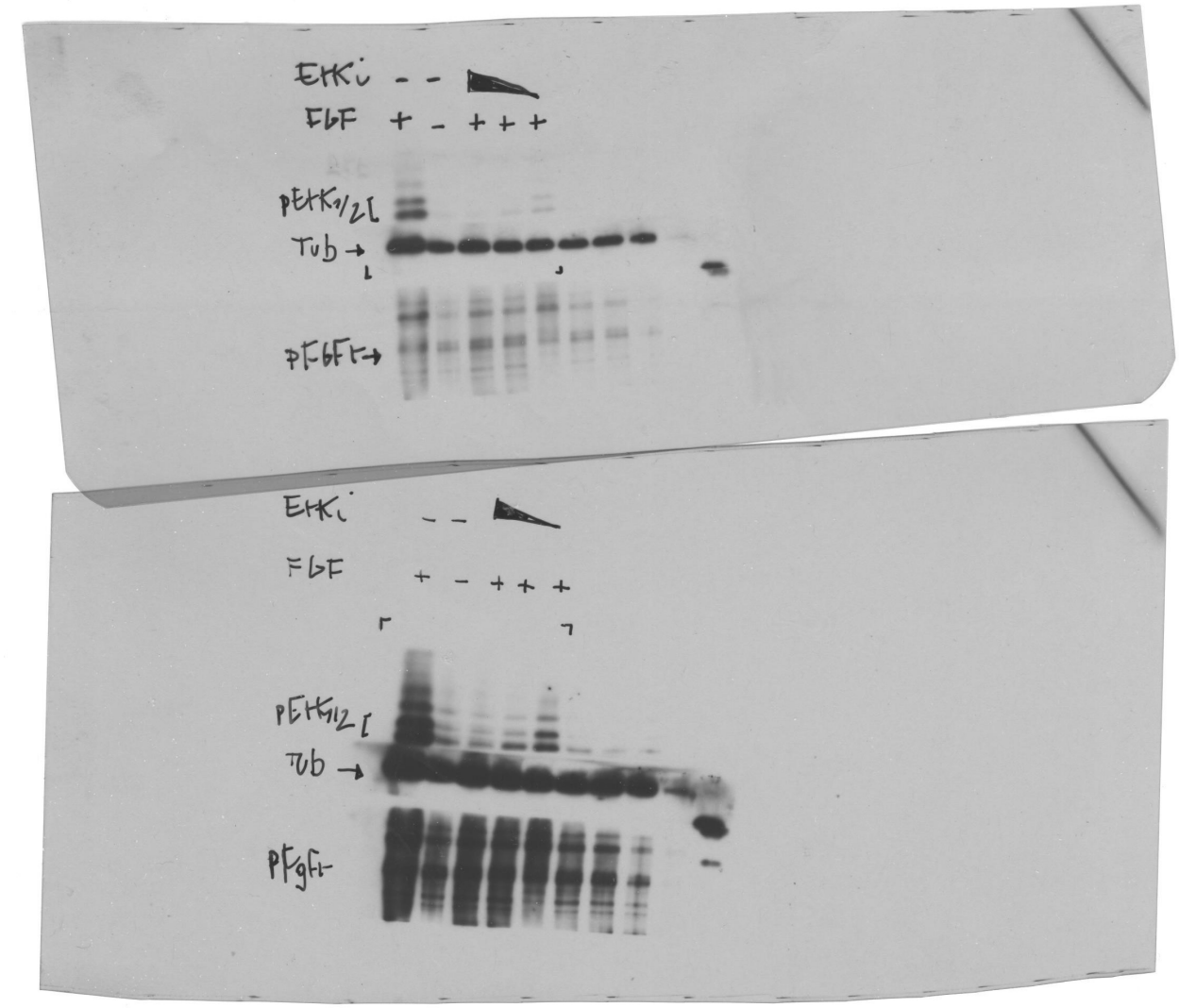

SUPPLEMENTARY FIGURE S10

Fig. S10. ERK1/2 inhibition blocks bFGF-induced mammary branching. Raw western blot data of effects of SCH772984 treatment on phospho- and total ERK1/2 in response to FGF2 stimulation. Blots probed for pERK1/2, tubulin and pFGFR (top blot, short exposure; middle blot, long exposure) and for total ERK1/2 (bottom blot). Blots used for preparing Supplementary Figure S9.

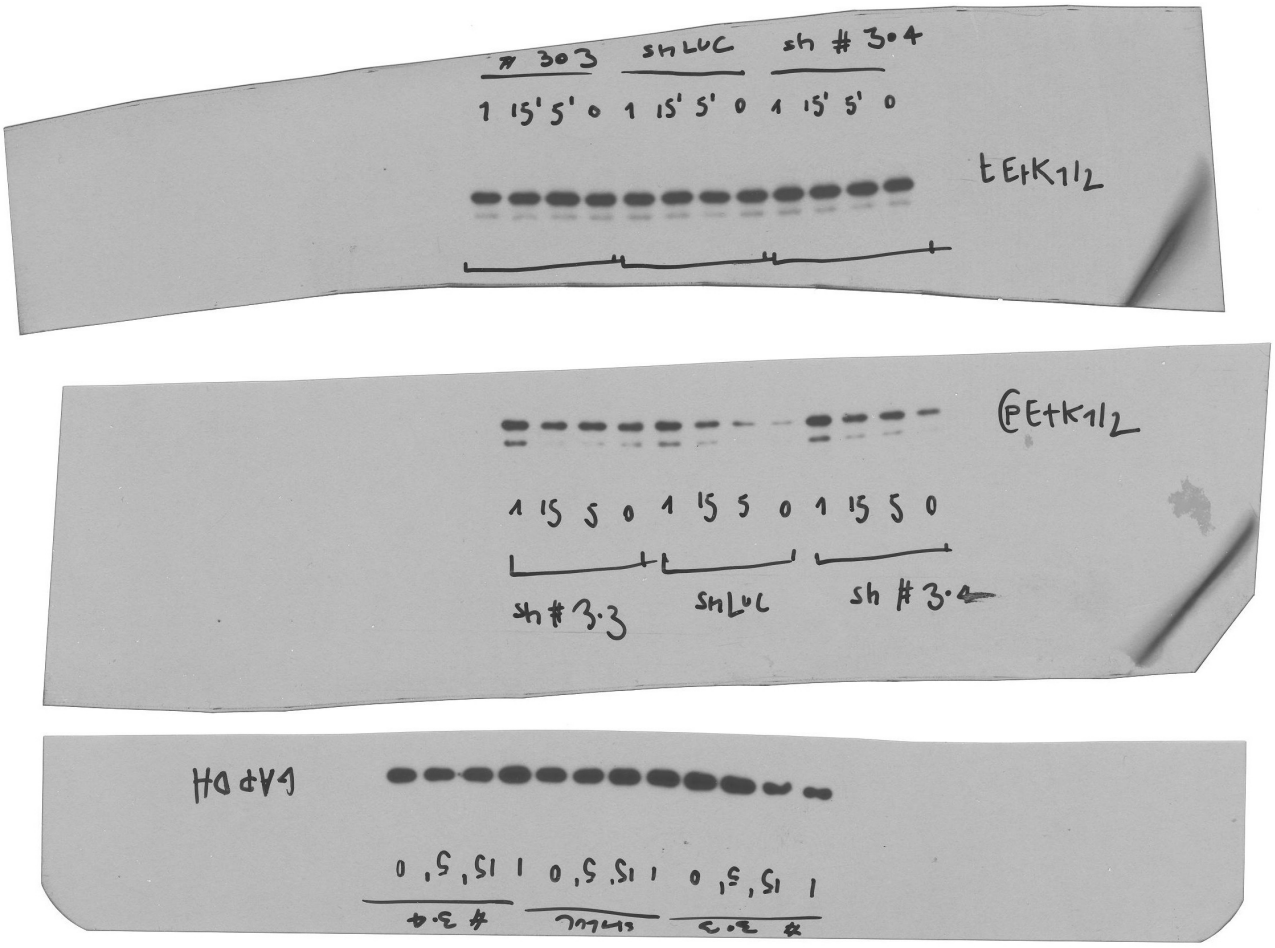

SUPPLEMENTARY FIGURE S11

Fig. S11. *Ptprb* knockdown enhances ERK1/2 phosphorylation. Raw western blot data of effects of *Ptprb* knockdown on ERK1/2 phosphorylation in response to FGF2 stimulation. Films of representative blots probed for total ERK1/2, phospho ERK1/2 and GAPDH are shown (blots used for preparing Figure 7B).

SUPPLEMENTARY TABLES

Table S1. Gene expression analysis comparing isolated TEBs vs ductal fragments. Data for 3756 genes with >1.5 fold differential expression between the two structures from two independent replicates each of which analysed TEBs and duct fragments from >100 animals.

Click here to Download Table S1

Table S2. Sybr green probes and TAQMan assays for quantitative real-time rtrPCR.

Gene	Unigene	TAQMan Assay
Actb	Mm.391967	Mm00607939_s1
Egfr	Mm. 8534	Mm00433023_m1
Erbb2	Mm. 290822	Mm00658541_m1
Fgfr1	Mm. 265716	Mm00438930_m1
Fgfr2	Mm. 16340	Mm00438941_m1
Igf1r	Mm. 275742	Mm00802831_m1

Gene	Unigene	Sybr Green probes
Actb	Mm.391967	Fwd: agcgcaagtactctgtgtgga
		Rev: gggccggactcatcgtact
Ptprb	Mm.37213	Fwd: acatttatggggcagtgcat
		Rev: gttccgcagtttctttgctc
Tek/Tie2	Mm.14313	Fwd: gacagtgctggagggagaag
		Rev: tccgcagagcagtcaattc

SUPPLEMENTARY REFERENCES

Britt, K. L., Kendrick, H., Regan, J. L., Molyneux, G., Magnay, F. A., Ashworth, A. and Smalley, M. J. (2009). Pregnancy in the mature adult mouse does not alter the proportion of mammary epithelial stem/progenitor cells. *Breast Cancer Res* **11**, R20.

Regan, J. L., Kendrick, H., Magnay, F. A., Vafaizadeh, V., Groner, B. and Smalley, M. J. (2012). c-Kit is required for growth and survival of the cells of origin of Brca1-mutation-associated breast cancer. *Oncogene* **31**, 869-83.